Journal of Materials & Manufacturing Technology

www.jmmt.reapress.com

J. Mater. Manuf. Technol. Vol. 2, No. 1 (2025) 42–53.

Paper Type: Original Article

Experimental Study and Analysis of Dynamic Belt Tension Design and Measurement in Driver-driven Pulley Systems

Victor Etok Udoh[1,*], White Akpan[2], Ndifreke Effeng[2]

[1]Department of Welding and Fabrication Engineering, Akwa Ibom State Polytechnic, IkotOsurua, Nigeria; ictor.ude@akwaibompoly.edu.ng.

[2] Department of Mechanical and Aerospace Engineering, University of Uyo, Nigeria.

Citation:

Received: 18 April 2024 *Revised: 25 May 2024* *Accepted: 14 November 2024*	Victor Etok, U., White, A., & Ndifreke, E. (2025). Experimental study and analysis of dynamic belt tension design and measurement in driver-driven pulley systems. *Journal of Materials & Manufacturing Technology, volume* (Issue), pp.

Abstract

Belt drive systems are an effective means for power transmission with light weight, low cost, quietness, and efficiency. The objective of this study was to accurately measure the tension dynamic situations in the belt drive and the time used during running. The materials used were of high-quality engineering materials, which ensured accurate tension measurements. They consisted of a frame, driving pulley, video camera, v-belt, driven pulley, mirror (calibrated), and AC motor. The stability and support for other components were provided by the frame. Recording of deflections on the belt drive system was done with the use of a video webcam, while the mirror reflected the tension and deflections in the belt. Motion was transmitted by the AC motor between the two pulleys. The blower positions were at minimum and midpoints. MATLAB workspace Algorithm was used for the analysis. The largest displacement values were recorded when the blower was at the minimum position. Values of 10mm, 10mm, 12mm, 11mm, 11mm, and 12mm produced corresponding load tensions of 10N, 10N, 8N, 9N, 9N, and 8N, with the operating time of 5 to 10 minutes, respectively. At mid-point, the displacement values decreased, and the belt tension values increased significantly within the same time frame. The values obtained at midpoint were 8mm, 10mm, 11mm, 10mm, and 9mm, which produced belt load tensions of 11N, 9N, 8N, 9N, and 10N. The indication is that the measurements of the belt tension system ensured an efficient operation of belt-driven systems. Proper tensioning improved performance and also helped extend the lifespan of other components.

Keywords: Experimental study, Dynamic belt tension, Measurement, Pulley systems, Deflections.

1 | Introduction

It is a well-known fact that the production sector is the prime mover of any nation. Therefore, the development of any country is born at the manufacturing table. However, there are several challenges that militate against having an efficient production system. In a typical engineering system, though attainment of

Corresponding Author: ictor.ude@akwaibompoly.edu.ng

https://doi.org/10.48314/jmmt.v2i1.42

100% efficiency is impracticable, which owes much to heat, friction, and other forms of losses, it is, however, our priority to constantly develop a system that could give a better output [1], [2]. Improvement in the efficiency of mechanical systems is rather inevitable if quality, affordability, and profit optimization are to be attained. Mechanical Engineering, among other applications involve transmission of power, which can be done through various means. The means here is tailored to several factors, which are to be considered before the choice is made, which are the centre distance between the driver and driven pulley, the financial implications, the level of efficiency, and the amount of power to be transmitted [3]. However, the important parameters to be considered when choosing a belt derive is the power to be transmitted, speed of the driver and the driven shaft, and speed reduction ratio. Furthermore, while gear drives are good for short centre distances and efficient transmission, belt drives stand out centre distance is required, which nonetheless gains its popularity due to the effectiveness of the system [4], [5]. Belt drives find application in conveyor belt systems, car engines, and many other applications. Belts which are: flat belt, V-belt, and synchronous belt. Belt drives involve the use of two or more pulleys connected with the help of a belt in tension. There are different types of belts, which are flat, V-belt, and synchronous belt. Belt drives can be classified as open belt drive, cone pulley drive, stepped cone pulley drive, quarter-turn belt drive, and compound belt drive [6]. However, power transmission is dependent on the velocity of the belt, the tension under which the belt is applied to the pulley, are of contact between the belt and the small pulley, and the condition under which the belt is used [7]. Additionally, for the efficiency of the machine to be improved, monitored, and extrapolations made at every point, it becomes important that certain parameters be known and found at every point along the production line. However, for this to be feasible, parameters such as tension on the belt must be found and monitored along the production line in order to enable the efficiency to be found [8]. Furthermore, tension in a broad sense is a force which acts along the length of the medium which acts along the length through a rope, when pulled in the opposite direction. Tension is a contact force that is initiated by the driver pulley with the aim of transmitting the power to the driven pulley [9]. However, in order to have a smooth transmission process and ensure that the output conforms to the laid-down specification, the belt must be properly tensioned. However, the first step in the transmission process is proper belt tensioning. This involves proper determination of the tension to be induced (carried) in the belt, and proper positioning of the belt to be able to run without slip or with limited vibration [10]. Also, while tension in a belt can be determined by a range of methods, none of these methods can account for the minor and sharp changes normally occasioned during operation in a belt drive system. Also, the present methods can only be used in static situations. To have a clear picture of the belt drive system, a rotating mechanism must be available, while the revolving belt drives the pulleys is monitored for possible displacements and deflections during transmission. Hence, the application of a mirror in detecting these deviations become important [11], as it allows for timely detection and evaluation of tension, with the help of a mirror. This allows for timely information gathering in order to ensure appropriate quality control measures when there is non- conformance. Mirrors have key properties that allow them to be used in reflective, radiation and other countless image capturing application [12], [13]. However, to construct a mechanical device that could measure the tensions in belt drives in dynamic situations involves measuring the deflection of the belt at mid-span of the belt and transmitting this signal using a camera placed against a calibrated mirror. Where the signal could be further processed with the help of a MATLAB workspace connected to the camera.

2|Materials and Methods

The materials employed in these include a calibrated mirror, a blower, a wooden board (base), a personal computer, a belt drive system, an electric motor, a camera, software packages, etc. The research work designed and produced a mechanical system for the detection of belt tension using a mirror, where efficiencies of belt drive systems could be evaluated.

2 | Materials and Methods

The materials employed in these include a calibrated mirror, blower, wooden board (base), personal computer, belt drive system, electric motor, camera, software packages, etc. The research work designed and produced a mechanical system for the detection of belt tension using a mirror, where efficiencies of belt drive systems could be evaluated.

2.1 | Principles of Operation of the Machine

The work involves the use of a calibrated mirror in determining the deflection of the belt drive system, after which the belt tension is calculated from the transmitted signal. A calibrated mirror is attached to the centre of the belt, where the deflection – the sag- can be read off with the help of the calibration. However, a camera is beamed against the mirror where a video recording of the sag at mid-span engagement with the mirror is recorded and fed into the MATLAB workspace, where the video is processed and decomposed into frames for further analysis. The corresponding values of tensions are evaluated, and a safe region is marked out. With this, warnings are triggered where efficiencies are found to fall below the safe value. Furthermore, belt tensions could then be calculated using appropriate equations. *Fig.1* below shows a detailed image conversion process for the determination of belt tension.

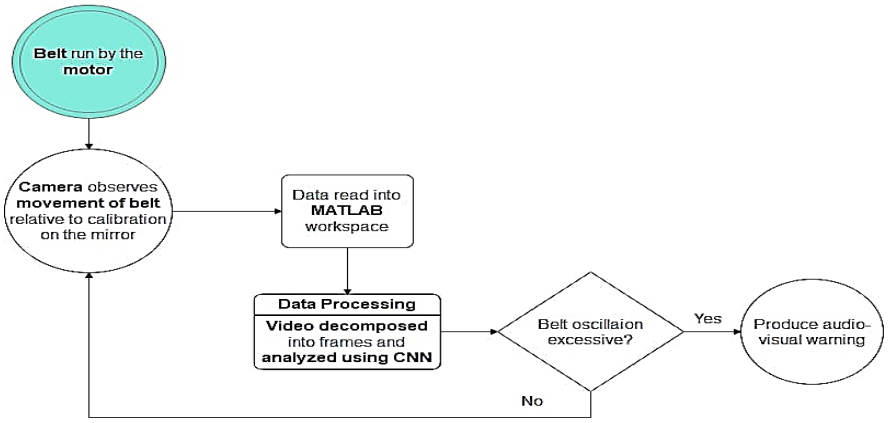

Fig. 1. Detailed image conversion process in the determination of belt tension.

2.2 | Design Analysis of the Machine

The design involves the deployment of a mirror in establishing tension of the belt system and also in imposing checks to ensure that the efficiencies of the belt system do not fall below the permissible value in order to ensure that the quality does not affect the final product produced in a typical industrial setting [14]. More so, the achievement of imposing checks is made possible by the use of a camera that records the belt sag at mid-span, thereby allowing extrapolation of this data using MATLAB workspace. The processes involved are as presented below:

I. Calibration of Mirror: This involves calibration of the plane mirror in order to account for variance in sag (vertical height) at mid-span during loading. This allows for accurate measurement of deflection.

II. Image capture: Image capture involves the use of a camera to record the movement of the belt at mid-span with reference to the mirror.

III. Image processing: this involves analysis of the recorded video with MATLAB workspace, where the images are decomposed into frames and thereafter used in imposing checks to ensure conformance to the laid down standard.

IV. Data analysis: the decomposed images were further analysed, thereby enabling the efficiencies as well as belt tension to be computed using appropriate equations.

V. Feedback system: this involves a programmable instruction issued to the system, which permits an audio/ visual warning when the efficiencies are found to fall below the threshold. Fig.2 shows the experimental setup of the system.

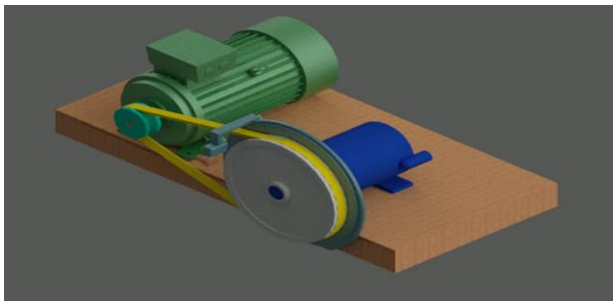

Fig. 2. Experimental setup.

The length of the belt can be calculated using *Eq. (1)*:

$$l_b = [(\pi d/2) + (\pi D/2) + (2lcc) + (D-d)^2/(4lcc)]. \quad (1)$$

$$= \pi/2(d+D) + 2lcc + (D-d)^2/4lcc, \quad (2)$$

where D is the diameter of the driven pulley, d is the diameter of the driver pulley, $L_{cc}$is the centre distance between the two pulleys, and l_b is the length of the belt. Velocity of the belt travel is given by *Eq. (3)*:

$$V_b = \pi D N_D/60. \quad (3)$$

where: N_D is the speed of rotation of the driven pulley and $\pi = 3.142$.

Velocity ratio can be found thus: the relationship of rotational speed between the driver and the driven and their diameters given by *Eq. (4)*:

$$DN_D = dNd. \quad (4)$$

Dividing both sides by D and thereafter by Nd gives

$$N_D/Nd = d/D. \quad (4)$$

$$\therefore \text{Velocity ratio} = N_D/N_d = d/D, \quad (5)$$

$$\text{Angle of contact}, \theta = 180 \pm 2 \text{ Arc Sin } [(D/2) - (d/2)]/lcc, \quad (6)$$

$$\text{gain}, \alpha \text{ can be found using}, \text{Sin}\alpha = (R+r)/lcc \quad (7)$$

However, *Eq (7)* can be rewritten as:

$$\theta = 180 \pm 2\alpha. \quad (8)$$

where R is the radius of the driven pulley, r is the radius of the driver pulley, and α is the arc of contact.

However, according to Euler's model, tensions at the ends of a stretched belt wrapped around a pulley satisfy the condition:

$$T_1/T_2 = e^{\mu\theta}, \quad (9)$$

$$2.3 \log (T1/T_2) = \mu\theta \text{Cosec}\beta. \quad (10)$$

where μ is the coefficient of friction, θ is the contact angle, T_1 is the tight side, and T_2 is the slack side.

Eq. (9) and *Eq. (10)* are used in calculating Tension in flat belt and V-belt, respectively. From *Eq. (9)*, work done and power transmitted by a belt can be calculated using *Eq. (11)*:

$$\text{Power transmitted} = (T1 - T2)\, V. \quad (11)$$

Also, it is worthy of note that when belts are set in motion, it generates a centrifugal force, known as centrifugal tension. At lower belt speeds (less than 10m/s), the centrifugal tension is very small, but at higher belt speeds (more than 10m/s), its effect is considerable and thus should be taken into account. This adds up to the tension on the tight and slack side as [15]:

$$T1t = T1 + T, \quad (12)$$

$$T2t = T2 + Tc, \quad (13)$$

$$Tc = mv. \quad (14)$$

where $T1t$ is the total tension in the tight side, $T2t$ is the total tension in the slack side, and Tc is the centrifugal tension. This transforms the formula for the ratio of tension to:

$$2.3 \log (T1t + T_C)/(T_{2t} - T_C) = \mu\theta. \quad (15)$$

It should be noted that the maximum tension is derived from the tight side of the belt (Ty), without consideration of centrifugal tension, but when centrifugal tension is considered,

$$Tmax = T_1 + T_C. \quad (16)$$

Additionally, when the power transmitted is maximum, 1/3 of the maximum tension is absorbed as centrifugal tension, hence,

$$T = 3T_C. \quad (17)$$

Consider a scenario when a belt is placed on pulleys. This generates a tension called Initial tension, which increases the tension in the tight side and decreases the tension in the slack side when the belt is set in motion, thus giving $T_1 - T_0$ and $T_0 - T_2$ as an increase in tension in the tight side and a decrease in tension in the slack side from the above could be found as.

$$T_0 = (T_1 + T_2)/2. \quad (18)$$

However, when consideration is made of centrifugal tension:

$$T_0 = (T_1 + T_2 + 2T_C). \quad (19)$$

The values obtained when the sag was at corresponding deflections of $1cm$ during the run time were given in equation 20, where the tension corresponding to these deflections at mid-span is the T_2.

$$\therefore T_2 = \frac{K}{L}. \quad (20)$$

3 | Experimental Set Up

The experimental setup is as shown in *Fig. 3*. An electric motor and a blower are mounted on a wooden board. Pulleys with grooves are fixed to the shaft of both the motor and blower. The electric motor is powered by the power source, which thereafter provides drive to the pulley attached to the shaft of the electric motor. The power from the electric motor then drives the blower with the help of the V-belt. However, the use of a blower here is to allow the system to have a typical industrial loading experience, where deductions could be made thereafter. However, a calibrated mirror is attached to the driven pulley, where the arc of contact of the belt could easily be read. A camera is also placed against the driven pulley, which records the belt movement– subsequently processed to have a finite value. The software product involves the use of MATLAB workspace to analyse the recorded data, with a programmable instruction that enables the feedback system. The tension of the belt is then computed. The experimental setup of the blower and V-belt pulley system is presented in *Fig. 3*.

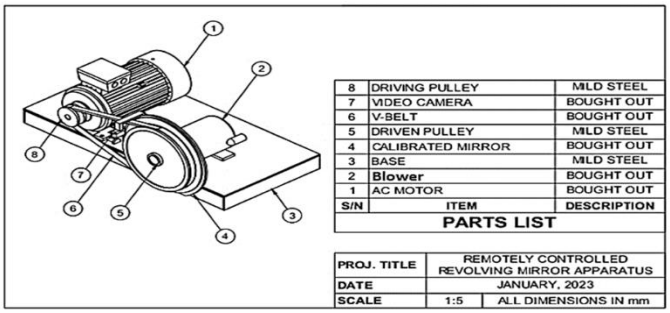

Fig. 3. Experimental setup showing part design.

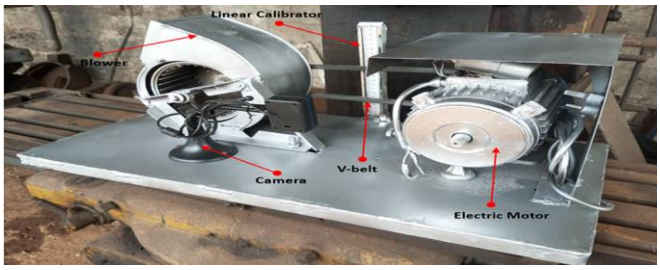

Fig. 4. Experimental set-up showing the blower and the V-belt pulley system.

4 | Discussion

The machine was manufactured using locally available materials and thereafter assembled. The International Standard Organisation recommendations were also adopted during the design and Quality specification of the model. The results are presented in *Figs. 3* to *Fig. 4* below.

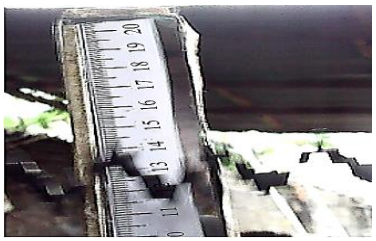

Fig. 5. Decomposed imagewhen blower was at mid position.

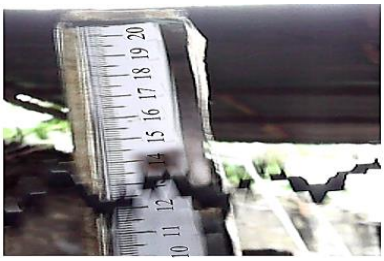

Fig. 6. A Decomposed image when the blower was at the maximum position.

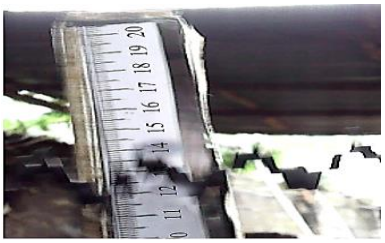

Fig. 7. Decomposed Image when Blower was at Mid position.

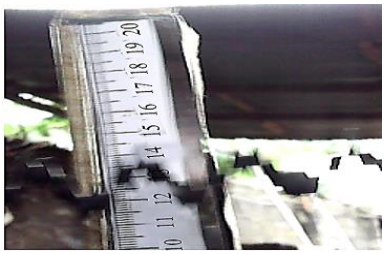

Fig. 8. Decomposed imagewhen blower was at the maximum position.

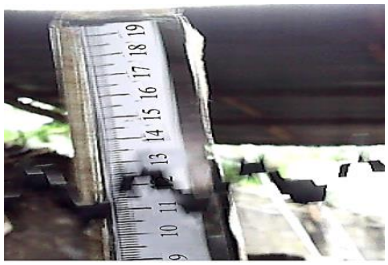

Fig. 9. Decomposed image when at minimum position.

Fig. 10. Decomposed image when the blower was at the maximum position blower was

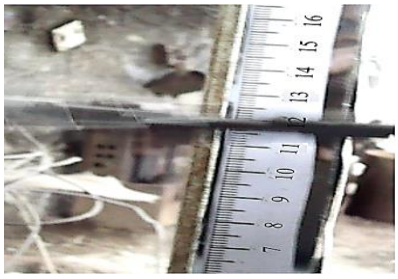

Fig. 11. A Decomposed image when the blower was at the maximum position.

Fig. 12. A Decomposed image when the blower was at the maximum position

Fig. 13. A Decomposed image when the blower was at the minimum position.

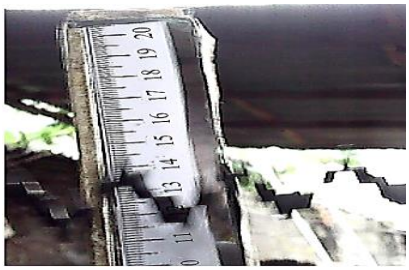

Fig. 14. A Decomposed image when the blower was at mid position.

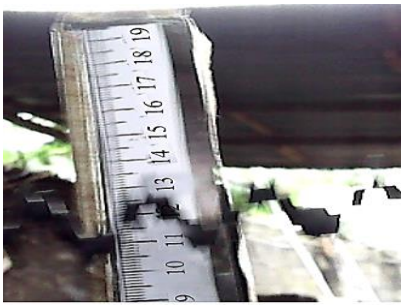

Fig. 15. A Decomposed Image when the blower was at the maximum position.

Fig. 16. A Decomposed Image when the blower was at the minimum position.

Table 1. Sag positions with corresponding tension and time at the minimum blower position.

Sag (mm)	Tension (N)	Time Operated (min)
10	10	5
10	10	6
12	8	7
11	9	8
11	9	9
12	8	10

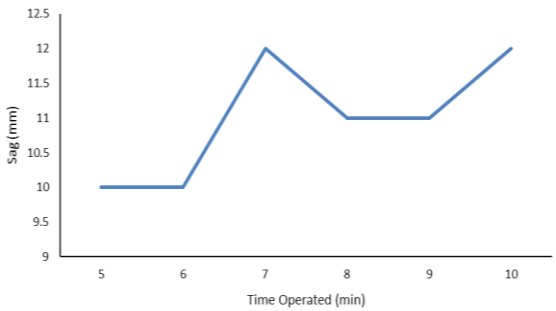

Fig. 17. Graph showing belt sag against operated time at minimum blower position.

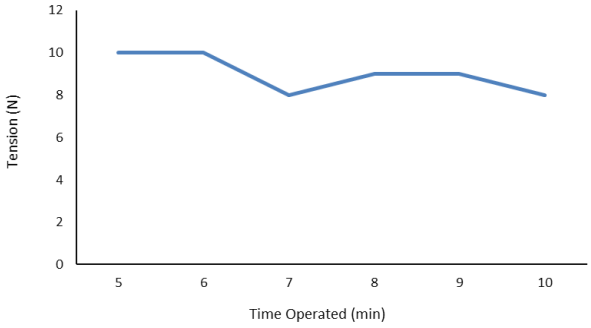

Fig. 18. Graph showing belt tension against operated time at the minimum blower position.

Table. 2. Sag positions with corresponding tension and time at the midpoint blower position.

Sag (mm)	Tension (N)	Time Operated (min)
8	11	5
8	11	6
10	9	7
11	8	8
10	9	9
9	10	10

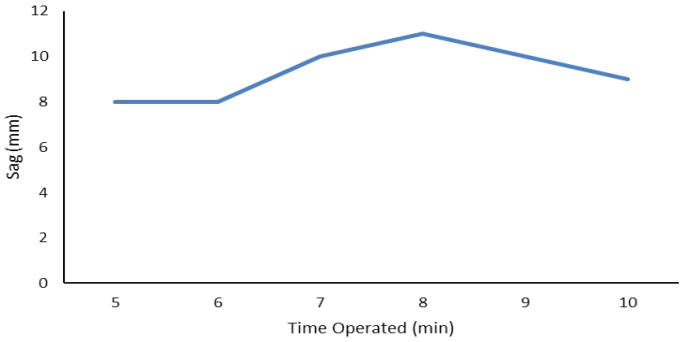

Fig. 19. Graph showing belt sag against operated time when the blower is at mid-span position.

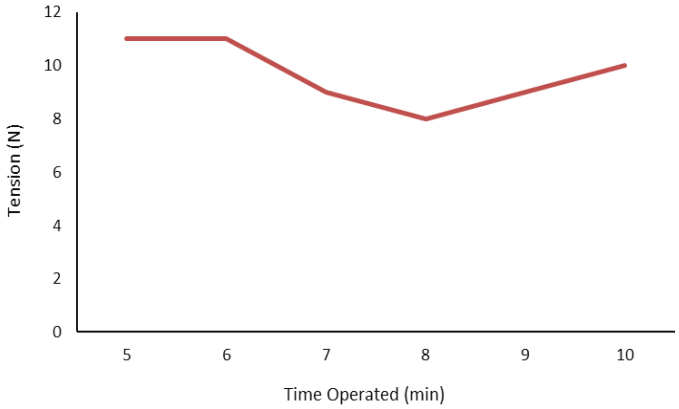

Fig. 20. Graph showing belt tension against operated time when the blower is at mid-span position.

4.1 | Discussion

The results of the research presented above are discussed herein. The system was designed to evaluate belt tensions in dynamic situations. The system was designed to monitor the belt sags and the corresponding time during run-time. This was made possible through video recording using a webcam, video decomposition, and

analysis of the resulting images with the help of a MATLAB workspace. The images generated using MATLAB workspace are shown in *Figs. 5* to *16*, respectively. Consequently, the Sag positions were obtained, with their corresponding time, while the belt tension was thereafter calculated using the derived *Eq. (20)*. These values are presented in *Table 1* and *Table 2,* respectively. However, the model has an adjustment at the blower, which allows the blower to be adjusted to multiple positions in order to allow for a better analysis of the effect of variations in belt tensions on the model. The blow stretched positions chosen were the maximum position, which is when the belt is at full stretch; the mid position, and the minimum position of the blower. The results are presented in the tables and figures above.

4.2 | Decomposition of the Video

The videos recorded with the help of the camera were decomposed into frames with the help of the MATLAB workspace and an algorithm presented in Appendix A. This is a result of the real-time operation of the belt drive system. These results of the analysis are presented in *Figs. 5* to *16*, respectively. However, the images presented in these Figures show the deflections (Sags) for the system when the blower positions were at minimum and midpoints, enabled by the adjustment provisions at the blower end. From the images in these Figures, it can be seen that sag positions when the blower was at the minimum adjustment position recorded large values compared to the values obtained when the blower positions were adjusted to the maximum and the mid-position. This means that, at maximum position, the belt tension increases, which is due to the increase in pulley centre distance, thus resulting in smaller values of sag. Furthermore, minimum positions recorded higher values. This further buttresses the fact that belt sag and the belt tension have an inverse relationship.

4.3 | Comparative Analysis of Belt Tensions and Belt Sags at Different Blower Positions

The results of the belt operation analyzed using MATLAB are presented in *Tables 1* and *2,* which correspond to the minimum and mid-position positions, respectively.

However, the largest Sag value is recorded in *Table 1,* which is when the blower is in the minimum position. The lowest value of sag was 10mm, which gave a belt tension of 10N when the belt was in operation for 5 minutes. Other values of sags were: 10mm, 12mm, 11mm, 11mm, and 12mm at tensions of 10N, 8N, 9N, 9N, and 8N, respectively. The operating times for this sag and tension values were 6 minutes, 7 minutes, 8 minutes, 9 minutes, and 10 minutes, respectively. The values from *Table 1* show two regions where the belt parameters remained unchanged. This was recorded when the time was 5 to 6 minutes and 8 to 9 minutes.

Table 2 shows the belt parameters when the blower was at mid-position. At mid-position, there was a remarkable decrease in the values for Sags, while there was an increase in values for belt tension with the same timeframe under consideration. The first value of sag was 8mm, which corresponds to belt tension values of 11N when the system was operated for 5 minutes. The succeeding values of sags were 8mm, 10mm, 11mm, 10mm, and 9mm. This corresponds to belt tension values of 11N, 9N, 8N, 9N, and 10N, when the system operated time was 6, 7, 8, 9, and 10 minutes, respectively. The belt parameters, however, remained unchanged during its transition from 5 to 6 minutes.

Comparatively, the values presented in *Table 1* and *Table* 2 show a trend: a decrease in sag with an increase in the centre distance of the pulley, which also leads to an increase in belt tension values.

4.4 | Deductions from the Graph

The relationships between belt tension against operated time and belt sag against operated time are shown in *Figs. 17-20*, respectively.

However, considering the behavior of the graphs of Belt Sags against Belt Tensions for the three test positions, the maximum sag values were obtained when the period of operation was 7 minutes and 10 minutes

in *Fig. 7* and *Fig. 8* minutes in *Fig. 9,* and *7* minutes and *10* minutes in *Fig. 11* which corresponds to the minimum position, the mid-position and the maximum position, respectively. Also, the behavior of the graph in *Fig.18*depicts the plastic deformation of the polymer. This shows clearly that the belt has exceeded the maximum permissible tension, which, if it is continuously operated at this condition, will lead to failure. *Fig. 17* and *Fig. 18* are graphs of Belt Tension against Time for minimum blower position and mid-position blower positions, respectively.

Belt displacement against tension in pulley drive systems is a critical issue that can lead to inefficiencies and potential system failures. When a belt becomes displaced from its intended position on a pulley, it can cause uneven tension distribution, leading to increased wear and tear on the belt and pulleys. This can result in decreased power transmission efficiency and ultimately, system breakdown.

5 | Conclusion

The findings from this study on experimental study and analysis of dynamic belt tension design and measurement in driver-driven pulley systems have provided valuable insights into the complex dynamics of belt systems. Through experimentation and analysis, the study has identified key factors that influence belt tension, such as pulley size, belt material, and operating conditions. One of the key takeaways from this study is the importance of maintaining proper belt tension in driver-driven pulley systems. It has been shown that inadequate tension can lead to slippage, reduced efficiency, and premature wear of the belt and pulleys. Furthermore, the study has also highlighted the need for accurate measurement techniques to monitor belt tension in real-time. Advances in sensor technology and data analysis can enable manufacturers to develop sophisticated monitoring systems that can provide valuable feedback on the performance of pulley systems. This real-time data can help operators make informed decisions to optimize belt tension and prevent costly downtime.

Acknowledgments

The authors express their sincere appreciation to the management and staff of Universal Textiles Mills Limited, Kano, Nigeria, for providing the opportunity and practical exposure during the Industrial Attachment Programme, which formed the basis of this study. The authors also acknowledge the contributions of previous researchers whose works informed this study, particularly in the areas of Jacquard weaving and textile design. Appreciation is extended to colleagues and mentors who provided guidance during the course of this research.

Funding

This section indicates any support that is not included in the Author Contribution or Funding sections. This may include administrative and technical support or in-kind donations (e.g., materials used for experiments).

This research received no external funding.

Data Availability

We encourage all authors to make their research data available. Please indicate where the data supporting the reported findings can be found, including links to publicly archived datasets that were analyzed or generated during the study. If no new data were generated or if data are not available due to privacy or ethical restrictions, an explanation is still required. The data supporting the findings of this study are available within the article. Additional information can be requested from the corresponding author upon reasonable request.

Conflicts of Interest

The authors declare no conflict of interest. Authors must declare any personal circumstances or interests that could be considered to have an inappropriate influence on the presentation or interpretation of the reported research findings. Any role of funders in the design of the study, in the collection, analysis, or interpretation of the data, in the writing of the manuscript, or in the decision to publish the results must be disclosed in this section. If this is not the case, please indicate "Funders played no role in the design of the study, in the collection, analysis, or interpretation of the data, in the writing of the manuscript, or in the decision to publish the results."

References

[1] Rademaekers, K., Van der Laan, J., Smith, M., Van Breugel, C., & Pollitt, H. (2011). The role of market-based instruments in achieving a resource efficient economy. *International Institute for Sustainable Development (IISD), Winnipeg, Manitoba, Canada*, 34-37. https://op.europa.eu/en/publication-detail/-/publication/c3f85c88-ae2b-4835-9c17-1a4b8bb50e16

[2] Raghavendra, N. V., & Krishnamurthy, L. (2013). *Engineering metrology and measurements* (Vol. 1, No. 2). New Delhi: Oxford University Press. http://ndl.ethernet.edu.et/bitstream/123456789/57247/1/565.pdf

[3] Fahriani, A. (2024). *Needs Analysis of English For Specific Purpose In Merdeka Belajar Curriculum at SMKN 2 Purwokerto* (Doctoral dissertation, Doctoral Dissertation, State Islamic University). https://repository.uinsaizu.ac.id/26053/1/Akhida%20Fahriani_Needs%20Analysis%20of%20English%20for%20Specific%20Purpose%20in%20Merdeka%20Belajar%20Curriculum.pdf

[4] Raji, N. A., Erameh, A. A., Yussouff, A. A., & Durojaye, R. O. (2016). Response surface methodology approach for transmission optimization of V-Belt drive. *Modern mechanical engineering*, *6*(1), 32–43. http://dx.doi.org/10.4236/mme.2016.61004

[5] Madu, K. (2018). Estimation of the power capacity of a belt in a fan-motor assemblage, under a given allowable stress. *Equatorial journal of computational and theoretical science*, *2*(2), 16–20. https://d1wqtxts1xzle7.

[6] Zhai, G., Liang, Z., & Li, M. (2019). Study on the optimization model of a flexible transmission. *Mathematical Problems in Engineering*, *2019*(1), 5084573. https://onlinelibrary.wiley.com/doi/pdf/10.1155/2019/5084573

[7] Werbińska-Wojciechowska, S., & Winiarska, K. (2023). Maintenance performance in the age of Industry 4.0: A bibliometric performance analysis and a systematic literature review. *Sensors*, *23*(3), 1409. https://doi.org/10.3390/s23031409

[8] Sullivan, G., Pugh, R., Melendez, A. P., & Hunt, W. D. (2010). *Operations & maintenance best practices-a guide to achieving operational efficiency (release 3)* (No. PNNL-19634). Pacific Northwest National Laboratory (PNNL), Richland, WA (United States). https://www.osti.gov/servlets/purl/1034595

[9] Song, G., Shen, Y., Chandrashekhara, K., Breig, W. F., Klein, D. L., & Oliver, L. R. (2003). *Thermal-mechanical finite element analysis of V-ribbed belt drive operation* (No. 2003-01-0925). SAE Technical Paper. https://www.jstor.org/stable/44741351

[10] Manin, L., Michon, G., Remond, D., & Dufour, R. (2009). From transmission error measurement to pulley–belt slip determination in serpentine belt drives: Influence of tensioner and belt characteristics. *Mechanism and Machine Theory*, *44*(4), 813-821. https://doi.org/10.1016/j.mechmachtheory.2008.04.003

[11] Guo, X., Liu, X., Zhou, H., Stanislawski, R., Królczyk, G., & Li, Z. (2022). Belt tear detection for coal mining conveyors. *Micromachines*, *13*(3), 449. https://doi.org/10.3390/mi13030449

[12] Wagner, H. J., Douglas, R. H., Frank, T. M., Roberts, N. W., & Partridge, J. C. (2009). A novel vertebrate eye using both refractive and reflective optics. *Current Biology*, *19*(2), 108-114.. https://www.cell.com/current-biology/fulltext/S0960-9822(08)01621-7

[13] Dobrovolny, L. (2015). *Current Trends in Spectral Reflectance Imaging Techniques: A Qualitative Approach to the Investigation and Documentation of Building Materials* (Doctoral dissertation, Columbia University). https://doi.org/10.7916/D8ST7PC9

[14] Ikpe, A., Ekanem, I. I., & Ikpe, A. E. (2024). A comprehensive study of the principles and trends in ac circuits: essential component in electro-mechanical systems and industries. *Intelligence modeling in electromechanical systems*, *1*(1), 17–38. https://doi.org/10.48314/imes.v1i1.22

[15] Chaudhari, H. S., Pokhrel, S., Saha, S. K., Dhakate, A., & Hazra, A. (2015). Improved depiction of Indian summer monsoon in latest high resolution NCEP climate forecast system reanalysis. *International journal of climatology*, *35*(10). https://openurl.ebsco.com.